文章编号 1674-2915(2011)04-0397-07

Single-pulse CO_2 laser frequency doubler based on GaSe and $GaSe_{0.7}S_{0.3}$ single crystals

TARASENKO V F[1], SITNIKOV A G[1], PANCHENKO A N[1], TEL´MINOV A E[1], GENIN D E[1], LI Dian-jun[2], ZHANG Lai-ming[2], JIANG Ke[2], XIE Ji-jiang[2], SARKISOV S Yu[3], BEREZNAYA S A[3], KOROTCHENKO Z V[3], KAZAKOV A V[3]

(1. *Institute of High Current Electronics SB RAS, Tomsk* 634055, *Russia*;
2. *State Key Laboratory of Laser Interaction with Matter, Changchun Institute of Optics, Fine Mechanics and Physics, Chinese Academy of Sciences, Changchun* 130033, *China*;
3. *Semiconductor Materials Science Laboratory, Siberian Physical and Technical Institute of Tomsk State University, Tomsk* 634034, *Russia*)

Abstract: An efficient CO_2 laser at 10.6 μm pumped by a generator with an Inductive Energy Storage(IES) generator and a Semiconductor Opening Switch(SOS) was described. Theoretical evaluation and experimental results on the second harmonic generation in GaSe and $GaSe_{0.7}S_{0.3}$ nonlinear crystals pumped by the laser were presented. Results show that for GaSe crystal, the maximum energy conversion efficiency is 0.38% at the energy of the incident radiation of 180 mJ, and the peak power of converted radiation is about 8 kW.

Key words: GaSe; $GaSe_{0.7}S_{0.3}$; single pulse CO_2 laser; frequency doubler

基于 GaSe 和 $GaSe_{0.7}S_{0.3}$ 单晶的单脉冲 CO_2 激光倍频器

TARASENKO V F[1], SITNIKOV A G[1], PANCHENKO A N[1], TEL´MINOV A E[1], GENIN D E[1], 李殿军[2], 张来明[2], 姜 可[2], 谢冀江[2], SARKISOV S Yu[3], BEREZNAYA S A[3], KOROTCHENKO Z V[3], KAZAKOV A V[3]

(1. 俄罗斯科学院 西伯利亚分院 强电流研究所,托木斯克 634055,俄罗斯;
2. 中国科学院 长春光学精密机械与物理研究所,激光与物质相互作用国家重点实验室,吉林 长春 130033;
3. 托木斯克州立大学 西伯利亚物理技术研究所,半导体材料科学实验室,托木斯克 634034,俄罗斯)

收稿日期:2011-04-11;修订日期:2011-06-13

基金项目:supported by the Federal Target Program "The scientific and Scientific-pedagogical Personnel of Innovative Russia"(No. 02.740.11.04444); Russian President Grant(SS4297.2010.2).

摘要:描述了使用电感储能发生器和半导体转换开关泵浦的工作波长为 10.6 μm 的高效 CO_2 激光器。给出了激光泵浦的非线性晶体 GaSe 和 $GaSe_{0.7}S_{0.3}$ 的二次谐波振荡的实验数据和理论估算结果。结果显示,GaSe 晶体在输入能量为 180 mJ 时,最大能量转换效率为 0.38%,倍频激光的峰值功率为 8 kW。

关 键 词:GaSe; $GaSe_{0.7}S_{0.3}$; 单脉冲 CO_2 激光; 倍频器

中图分类号:TN248.2 文献标识码:A

1 Introduction

An efficient high-power short-pulse CO_2 laser with an inductive energy storage generator and a semiconductor opening swich on the basis of SOS-diodes was tuned to generate TEM_{00} mode at the wavelength of 10.6 μm. The inductive energy storage generator easily allows to form a laser pulse with the short spike about 50 ns in duration (FWHM) and 1 μs tale.

In order to demonstrate the possibility to obtain coherent radiation at other wavelengths, we employed Second Harmonic Generation (SHG) process in nonlinear crystals. At our disposal we had centimeter-size GaSe and $GaSe_{0.7}S_{0.3}$ crystals which were well known to be efficient nonlinear crystals for mid IR and terahertz range conversion [1-3].

2 Theory

To set up the frequency doubler for our CO_2 laser, first of all we performed a choice of nonlinear crystals and type of interaction. The phase-matching curves were obtained by using dispersion relations from [4] for GaSe and from [5] for GaSeS (see Fig. 1).

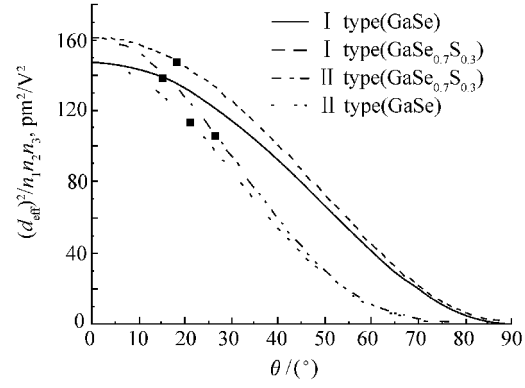

Fig. 1 Internal phase-matching angles for SHG in GaSe and $GaSe_{0.7}S_{0.3}$ crystals on I and II types of interaction. The dispersion relations from [4] and [5] were used.

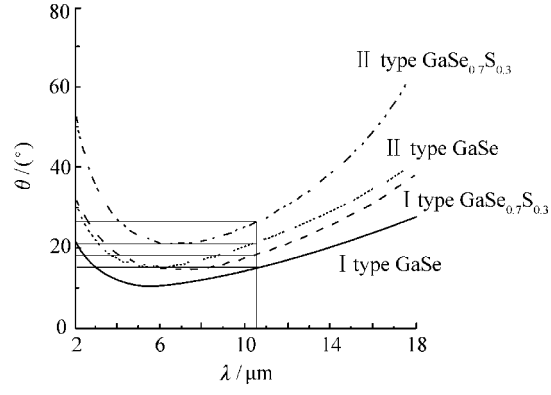

Fig. 2 Merit factors for GaSe and $GaSe_{0.7}S_{0.3}$ crystals on I and II types of interaction. The dots represent points related to phase-matching angles.

The SHG output power is proportional to the merit factors, plotted in Fig. 2. According to Fig. 2, the I type of interaction in both crystals requires lower phase-matching angles and corresponds to higher merit factors. When calculating curves in Fig. 2, we assumed that d_{22} component of nonlinearity of the second order for both crystals is equal to 54 pm/V.

Efficient nonlinearities depend on the polarization and orientation of interacting beams and are expressed as $d_{eff} = -d_{22} \times \cos\theta \times \sin 3\varphi$ and $d_{eff} = d_{22} \times \cos^2\theta \times \cos 3\varphi$ for the first and second types of interaction, respectively.

According to the above calculations, the I type of interaction is more efficient, so we performed our experiments in this configuration. The polarization of

the laser was vertical and the nonlinear crystals were rotated around vertical axis for phase-matching.

Calculation of the second harmonic radiation power P_{SHG} was made on the assumption of low conversion efficiency without depletion of the pumping power by using the well-known relation:

$$P_{SHG} = \frac{2\pi^2 d_{eff}^2 d^2 P_{CO_2}^2}{\varepsilon_0 c n_{CO_2}^2 n_{SHG} \lambda_{SGH}^2 S} \mathrm{sinc}^2\left(\frac{|\Delta k| d}{2}\right), \quad (1)$$

where d is the length of crystal, P_{CO_2} is an emission power of CO_2 laser, n_{CO_2}, n_{SGH} are refractive indexes at a wavelength of CO_2 laser and second harmonic, respectively, S is cross-sectional area of the laser beam, c is the speed of light, ε_0 is a dielectric constant and Δk is the wave detuning.

Thus, the estimations made predict that higher efficiency of SHG in $GaSe_{0.7}S_{0.3}$ can be expected. On the other hand, the real nonlinearity in these crystals can be lower than that in GaSe. In our experiments, we achieved higher conversion efficiency in pure GaSe, but these crystals were thicker.

3 Experimental technique and measurement procedure

The high-power single-pulse CO_2 laser pumped by the generator with semiconductor opening switch based on SOS-diodes [6] was used in our experiments for pumping crystals at the wavelength of 10.6 μm. Schematic diagram of the laser is shown in Fig. 3.

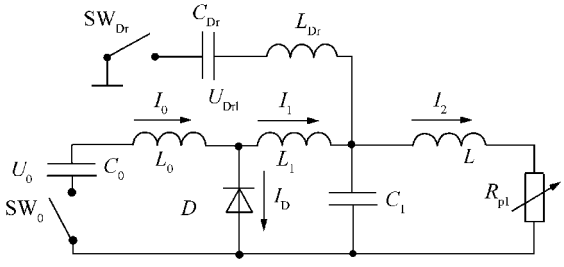

Fig. 3　Pumping scheme of CO_2 laser: R_{pl} is discharge resistance; SW_0 and SW_{Dr} are spark dischargers; $C_0 = 70$ nF is storage capacitor; $C_1 = 2.45$ nF is peaking capacitor; $C_{Dr} = 10$ nF is a capacitor for the forward pumping of SOS diodes; $L_0 = 24.5$ nH, $L_1 = 11$ nH, $L_{Dr} = 3.1$ μH are inductances of the circuits; U_0 and U_{Dr} are charging voltages; I is currents in the circuits.

The pump generator included the main and auxiliary circuits. The main circuit consisted of a storage capacity C_0 and an inductance L_0. The auxiliary circuit was used for preliminary forward pumping of SOS diodes and included a capacitor C_{Dr} and an inductance L_{Dr}. The energy stored in the auxiliary circuit was 2 J. In the laser, we used ten SOS-50-2 diodes positioned parallel to the peaking capacitors. The gas-discharge gap was preionised by the radiation from 72 spark gaps uniformly positioned from both sides of the anode, which were triggered by pulse charging of the peaking capacity C_1. The generator could operate both in the IES regime and a conventional LC generator. In the latter case, the capacitor C_{Dr} was not charged. The active laser volume V was 2 cm × 2 cm × 70 cm.

The laser output energy was measured by using an OPHIR calorimeter with FL-250A or PE-50BB sensors. The laser pulse waveforms were measured with a Ge-Au photoresistor of the FSG-33-3A1 type. Electrical signals were recorded with a TDS-3034 digital oscilloscope.

Optical cavity was formed by a Cu mirror and a TlBr plate. In the radiation conversion experiments, optical cavity includes a totally reflecting aluminum mirror with a radius of curvature 5 m and a plate of TlBr. Polarized radiation was obtained by using a NaCl plate placed at the Brewster angle between the laser mirrors. In order to form single-mode laser radiation, an aperture with a diameter of 7 mm was introduced into the laser optical cavity.

A SHG experiment was carried out as follows. The laser beam radiates on the crystal at 10.6 μm. To cut radiation SHG at a wavelength of 5.3 μm from transmitted through the crystal laser radiation, a sapphire filter was used. The coefficient of transparency of the filter at a wavelength of 5.3 μm is

measured to be 43%.

4 Experimental results and discussion

4.1 Laser operation

Comparison of laser excitation by different generators is shown in Fig. 4(a). A sharp cutoff of the current through the semiconductor diodes begins 25 ns after the start of the storage capacitor discharge shown in Fig. 4(b). During this time, the energy portion $E_L = L_0 I^2/2$ (where I is the amplitude of the cutoff current) is transferred to the IES (inductance L_0). The current through the diodes completely ceases after 75 ns, during which the energy dissipated in them reaches 6 J. At the cutoff instant, the current in the IES switches to charge the peaking capacitors. As a result, the IES for the time of ~10 ns charges the capacity C_1 to a voltage exceeding 70 kV, thus forming a high-voltage pre-pulse across the laser gap. After the laser gap breakdown, the residual IES current is summed with the current I_1 flowing through the peaking capacitor, which provides a

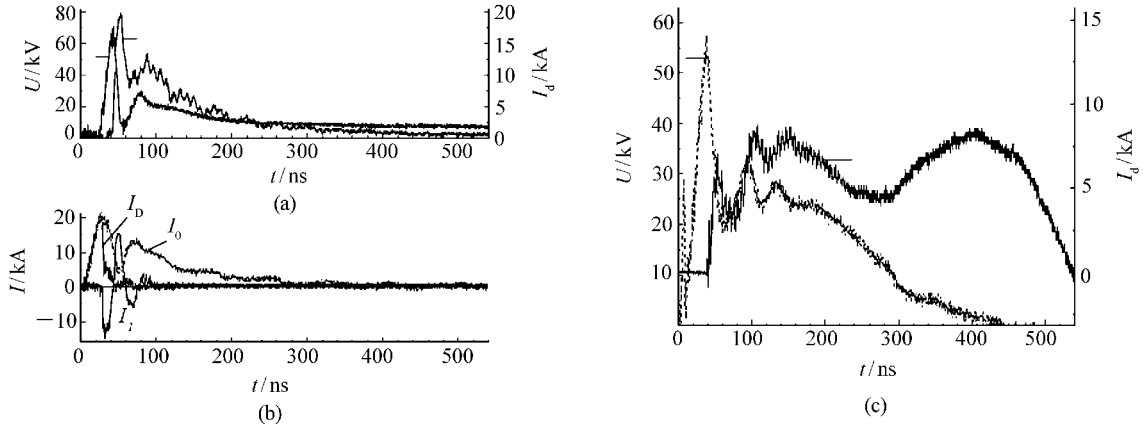

Fig. 4 Oscillograms of voltage pulses across the laser gap (U), current in the laser gap (I_d), current through the diodes (I_{SOS}), and currents in the circuits of the storage (I_0) and peaking (I_1) capacitors. The He:CO_2:N_2 = 3:1:1 mixture at $p \approx 101$ kPa was pumped by a generator with an SOS ((a), (b); I = 20 kA, E_L = 5 J) and an LC generator (c). The charging voltage of the storage capacitor is U_0 = 36 kV.

rapid increase in the discharge current and ensures the formation of a short high-power pump pulse. Then, the main part of the energy stored in the capacitor C_0 is deposited to the medium. The high overvoltage and the fast increase in the current, as this occurred in Ref. [6-9], allow formation of a stable volume discharge in CO_2 laser mixtures with high pressures and large concentrations of the molecular component. It is seen from the shape of the discharge current pulse (Fig. 4(a)). Approximately 120 ns after the pumping start, the current in the laser gap begins to exponentially decrease and the discharge extinguishes after the next ~500 ns. In this process, similar to the case with HF (DF) lasers, the storage capacitor can be discharged incompletely. The radiation pulse also contains a short peak with a half-height duration of 40 – 50 ns and a peak power of up to 45 MW, which is followed by a tail whose duration depends on the working mixture composition. In the mixture He: CO_2:N_2 = 3:1:1, the total laser pulse duration is ~1 μs, and its first peak contains 35% of the radiation energy. With increasing the molecular component concentration in the mixture or replacement of He by H_2, the part of the radiation energy in the first peak increases to 70% and the pulse duration decreases to 700 ns.

If the laser is pumped with the use of an LC

generator(Fig. 4(c)) , the peaking capacitor C_1 is charged only from the storage capacitor, which increases the rise time of the voltage across the laser gap to ~ 40 ns and decreases the laser gap breakdown voltage to 57 kV; the amplitude of the first pump peak simultaneously decreases twofold. Therefore, the energy in the first peak of the laser pulse decreases and the first peak duration increases. In addition, the switching off of the SOS leads to a loss of the discharge stability. In 250 ns after the laser gap breakdown, one observes a sharp increase in the current and a decrease in the laser gap voltage, which is typical of the transition of the volume discharge to the spark stage. In all the studied gas mixtures, with decreasing the charge voltage of the storage capacitor of the *LC* generator, the discharge contraction occurs 20 – 100 ns after the laser gap breakdown, which leads to a sharp decrease in the laser radiation energy. When the CO_2 laser is pumped by an *LC* generator, the voltage across the laser gap in the quasi-steady-state stage of the discharge noticeably increases. In the case of an IES, at maximum U_0, approximately half the energy is deposited to the active medium at the optimum parameter $E/p < 0.1\ \mathrm{V \cdot cm^{-1} \cdot Pa^{-1}}$, where E is the electric field strength [10].

In the case of an *LC* generator, the main energy contribution is made at $E/p \approx 0.15\ \mathrm{V \cdot cm^{-1} \cdot Pa^{-1}}$. An increase in E/p and the development of instabilities in the volume discharge noticeably decrease the lasing efficiency. For the conditions of Fig. 4, at $U_0 = 36$ kV, the energy deposited to the active medium is 31 J. With the use of the IES, the lasing energy is $Q = 6.2$ J, which corresponds to the internal efficiency(with respect to deposited energy) of the CO_2 laser $\eta_{int} = 20\%$, while electrical efficiency(with respect to stored energy) is as high as $\eta_0 = 14\%$. In the case of the *LC* generator, $Q = 2$ J and η_{int} does not exceed 7%.

4.2 Radiation conversion

Peak radiation power at maximal laser output (45 MW) is very high for nonlinear crystals because their damage threshold was measured to be not higher than 25 $\mathrm{MW/cm^2}$. Therefore working mixture of the $H_2 : CO_2 : N_2 = 2 : 4 : 1$ composition at a total pressure of 0.7 atm was used. In this case, the laser energy was 180 mJ. The laser pulse waveform is shown in Fig. 5. As in the case of He containing mixture, duration of the first peak was 50 ns(FWHM) and about 50% of the total energy was emitted in that peak. Measurement of the laser beam intensity profile shows that the profile is consistent with a Gaussian with a beam radius of 3 mm by the level of intensity e^{-2}.

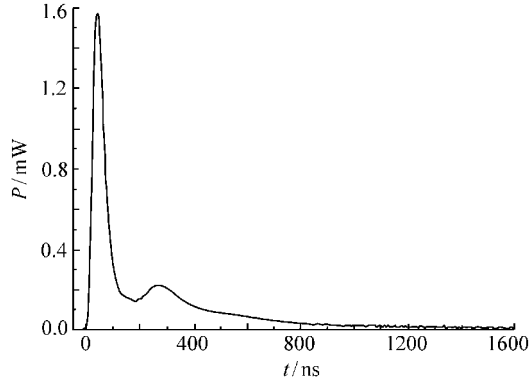

Fig. 5　Waveform of laser pulse power.

In the case(see curve 1) of the Fig. 6, the crystals allow to obtain radiation at 5.3 μm via I-type SHG process with considerable power even

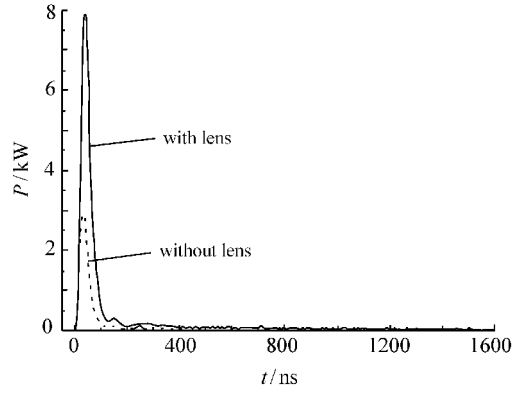

Fig. 6　Temporal behaviour of SHG radiation power for GaSe

without focusing of the pump radiation. The specific laser energy on the crystal surface was 2 J/cm^2. According to Eq. (1), the increase of the incident laser power should result in higher conversion efficiencies. Laser radiation was focused on the crystal by using NaCl lens with $f=234$ mm. Distance from the lens to the crystal L_d is 12 cm. In this case, peak power of the converted radiation was doubled and reached 8 kW for GaSe(see curve 2).

Fig. 7 depicts power conversion efficiency for GaSe calculated as the ratio between power of converted radiation and laser power in the same instant $=P_{SHG}/P_{las}$ obtained with a lens. It is seen that the maximal conversion efficiency is observed during first ~200 ns of the laser pulse. The efficiency was maximal during the laser pulse and was as high as 0.5%. Note that radiation conversion was observed during the whole laser pulse including its tale. However, efficiency was lower by one order of magnitude. Maximal energy conversion efficiency obtained in our experiments reached 0.38%. From 180 mJ of the incident radiation 0.7 mJ at a wavelength of 5.3 μm was obtained.

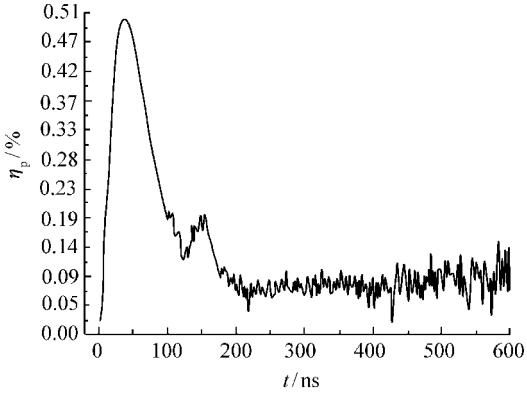

Fig. 7 Power conversion efficiency for GaSe crystal obtained with the lens.

We also measured the dependences of SHG output power on azimuth angle φ(see Fig. 8) and on incidence angle θ(see Fig. 9) for GaSe crystal. As is seen from Fig. 6, azimuth angle corresponding to the maximum SHG power is measured to be 34°.

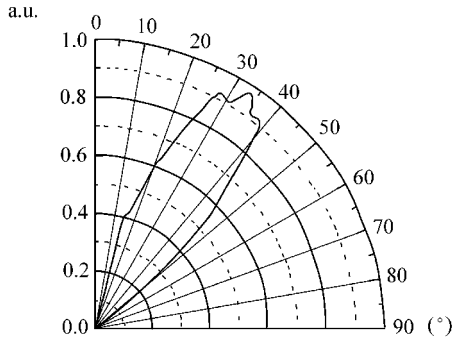

Fig. 8 Measured dependence of SHG output power on azimuth angle φ for GaSe.

Calculated and experimental angular dependences of the converted radiation power are in good match. The measured synchronism angle is 44.8°, and the calculated one is 44.5°. Widths at half maximum of the experimental and theoretical angular dependences of the SHG power were equal to 1.1°(see Fig. 9).

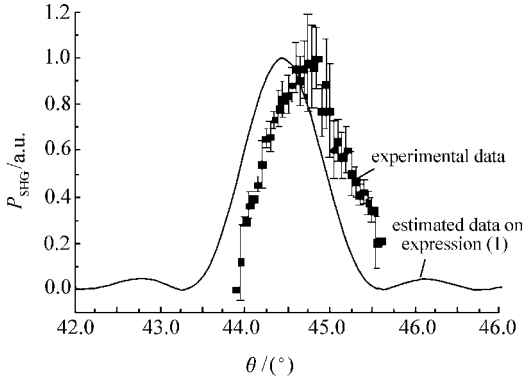

Fig. 9 Dependence of SHG output power on incidence angle θ for GaSe

Unfortunately, the SHG power for $GaSe_{0.7}S_{0.3}$ was not measured due to low energy resolution of the experimental apparatus. We estimates that the SHG power was about one order of magnitude lower than that for GaSe. Low SHG power for $GaSe_{0.7}S_{0.3}$ corresponds to theoretical estimation by using Eq. (1). $GaSe_{0.7}S_{0.3}$ crystal had a length of $d=3.7$ mm as compared to 10 mm for GaSe crystal. The efficiency is proportional to the d^2 resulting in one order effi-

ciency decrease for three-fold lower crystal thickness.

Comparison of the SHG efficiency in $GaSe_{0.7}S_{0.3}$ and GaSe crystals should be made either with the crystals with the same length, or with increased conversion efficiency, such as shorter laser pulses. In our further experiments, we plan to convert emission lines of the CO_2 laser into a THz range.

5 Conclusions

An efficient CO_2 laser pumped by a generator and a semiconductor opening switch was developed. The experiments of radiation conversion at 5.3 μm in nonlinear GaSe and $GaSe_{0.7}S_{0.3}$ crystals were performed.

References:

[1] SARKISOV S Yu, NAZAROV M M, SHKURINOV A P, *et al.*. $GaSe_{1-x}S_x$ and $GaSe_{1-x}Ts_x$ solid solutions for terahertz generation and detection [C] In Proceedings of the 34th International Conference on Infrared Millimeter and Terahertz Wave (IRMMW-THz-2009), Busan, Korea, 21-25 Sept. 2009.

[2] DAS S, GHOSH C, VOEVODINA O V, *et al.*. Modified GaSe crystal as a parametric frequency converter [J]. *Appl. Phys. B.*, 2006, 82(1): 43-46.

[3] MANDAL K C, KANG S H, CHOI M, *et al.*. Ⅲ-Ⅵ chalcogenide semiconductor crystals for broadband tunable THz sources and sensors [J]. *IEEE J. Selected Topics Quantum Electron.*, 2008, 14(2): 284-288.

[4] VODOPYANOV K L, KULEVSKII L A. New dispersion relationships for GaSe in the 0.65-18 m spectral region [J]. *Opt. Commun.*, 1995, 118: 375-378.

[5] ALLAHVERDIEV K R, GULIEV R I, SALAEV E Yu, *et al.*. Investigation of linear and nonlinear optical properties of GaS_xSe_{1-x} crystals [J]. *Sov. J. Quantum Electron.*, 1982, 12(7): 1483-1485.

[6] PANCHENKO A N, ORLOVSKII V M, TARASENKO V F. Spectral characteristics of nonchain HF and DF electric-discharge lasers in efficient excitation modes [J]. *Quantum Electron.*, 2004, 34(4): 320.

[7] PANCHENKO A N, TARASENKO V F, TEL´MINOV E A. Efficient electric-discharge XeF laser pumped by a generator with an inductive energy storage [J]. *Quantum Electron.*, 2006, 36(5): 403-407.

[8] PANCHENKO A N, SUSLOV A I, TARASENKO V F, *et al.*. Laser on mixtures of nitrogen with electronegative gases pumped by a transverse discharge from a generator with inductive energy storage: Theory and experiment [J]. *Quantum Electron.*, 2007, 37(5): 433-439.

[9] ORLOVSKII V M, PANCHENKO A N, TARASENKO Y F. Electric-discharge high-peak-power CO_2 laser [J]. *Quantum Electron.*, 2010, 40(3): 192-194.

[10] LOBANOV A N, SUCHKOV A F, SOV J. Breakdown of the active medium in a CO_2 laser caused by its own radiation [J]. *Quantum Electron.*, 1974, 4(12): 1436-1442.

Author´s biography: TARASENKO V F (1946—), male, professor of Laboratory of Optical Radiation, Institute of High Current Electronics, Siberian Branch of the Russian Academy of Sciences. His main research field includes gas discharges with runaway electrons, UV and VUV spontaneous light sources, pulsed lasers on dense gases and applications. E-mail: alexei@loi.hcei.tsc.ru